Available online at www.elixirpublishers.com (Elixir International Journal)

Computational Chemistry

Elixir Comp. Chem. 91 (2016) 38077-38086

ISSN: 2229-712X

FTIR, FT-RAMAN, *AB INITIO* and DFT studies on 2-Methoxy-6-Methyl Pyridine

K.Sambathkumar[1,*] and G.Ravichandran[2]

[1] P.G.&Research Department of Physics, A.A.Govt.Arts College,Villupuram-605602.India.

[2] P.G.&Research Department of Chemistry, A.A.Govt.Arts College,Villupuram-605602.India.

ARTICLE INFO

Article history:

Received: 9 December 2015;

Received in revised form:

28 January 2016;

Accepted: 3 February2016;

Keywords

FTIR,

FT-Raman,

HOMO,

LUMO,

TED,

NMR,

MMP.

ABSTRACT

Theoretical studies were conducted on the molecular structure and vibrational spectra of 2-methoxy-6-methyl pyridine (MMP). The FT-IR and FT-Raman spectra of MMP were recorded in the solid phase. The molecular geometry and vibrational frequencies of MMP in the ground state have been calculated by using the *ab initio* HF (Hartree-Fock)/6-311+G(d,p) and density functional methods (B3LYP) invoking 6-311+G(d,p)/6-311++G(d,p) basis set. The optimized geometric bond lengths and bond angles obtained by HF method show best agreement with the experimental values. Comparison of the observed fundamental vibrational frequencies of MMP with calculated results by HF and density functional methods indicates that B3LYP is superior to the scaled Hartree-Fock approach for molecular vibrational problems. The difference between the observed and scaled wave number values of most of the fundamentals is very small. A detailed interpretation of the FT-IR and FT- Raman, NMR spectra of MMP was also reported. NBO analysis has been performed in order to elucidate charge transfers or conjugative interaction, the intra-molecule rehybridization and delocalization of electron density within the molecule.UV–vis spectrum of the compound was recorded and the electronic properties, such as HOMO and LUMO energies, were performed by time dependent density functional theory (TD-DFT) approach. Finally the calculations results were applied to simulated infrared and Raman spectra of the title compound which show good agreement with observed spectra.

Introduction

The pyridine derivatives have an important position in the heterocycliccompounds and are important in bactericidal, fungicidal, germicidal and pharmacological activities [1]. And they can be used as nonlinear materials and photochemicals. Pyridines are widely used in pharmacological and medical applications. Some of them show anesthetic properties and have been used as drugs for certain brain diseases [2-4]. Pyridine tagged oligosaccharides have been widely used for sensitive qualitative and quantitative analysis by high performance liquid chromatography with fluorescence detection [2]. Pyridine is used in preparation of cytidine analogs [5] and it is also immensely used as a reagent in analytical chemistry. The vibrational spectra of 6-methyl pyridine have been investigated by several authors [6-9]. Extensive research in the last decade has shown that organic compounds often possess a higher degree of optical non-linearity than their inorganic counterparts. The literatures [10-12] supported by data banks [13-18] of various national and international journals an attempt has been madein this study to interpret the vibrational spectra of 2-methoxy-6-methyl pyridine (MMP) are performed by combining the experimental and theoretical information using density functional theory (B3LYP) and *ab initio* (HF) [19] to derive information about electronic effects and intramolecular charge transfer responsible for biological activity. The atomic charges, distribution of electron density (ED) in various bonding and antibonding orbitals and stabilisation energies, $E^{(2)}$ have been calculated by natural bond orbital (NBO) analysis. The NMR, HOMO-LUMO energy gap have been constructed at B3LYP/6-311++G(d,p) level to understand the electronic properties, electrophilic and nucleophilic active centres of MMP.

Experimental and Computational Details

Experimental

The pure sample of 2-methoxy-6-methylpyridine (MMP)was obtained from Lancaster Company, UK that is of spectroscopic grade and hence used for recording the spectra as such without any further purification. The FT-IR spectraof MP is measured in the BRUKER IFS 66V spectrometer in the range 4000 - 400 cm^{-1}. The FT-Raman spectrum of MMP and ABMP was also recorded in FT-RAMAN BRUKER RFS 100/S instrument equipped with Nd:YAG laser source operating at 1064 nm wavelength and 150 mW powers in the range 3500 - 50 cm^{-1}.

Computational

The initial geometry of MMP was optimized using the *ab initio* (HF) and B3LYP of GAUSSIAN 09W program package [20]. The vibrational frequency analysis was computed using *ab initio* (HF/6-311+G(d,p)) and B3LYP/6-311+G(d,p)/6-311++G(d,p) method to determine the nature of a stationary point found by geometry optimization.

Tele:+91 9994188861

E-mail addresses: sa75kumar@yahoo.co.in

Table 1. Optimized geometrical parameters of 2-methoxy-6-methylpyridine obtained by HF/6-31+G(d,p) and B3LYP/6-311G+(d,p)/6-311G++(d,p) methods and basis set calculations

Bond Length	Value (Å)			Exp[a]	Bond Angle	Value (°)			Exp[a]	Dihedral Angle	Value (°)		
	HF/ 6-31+ G(d,p)	B3LYP/ 6-311+ G(d,p)	B3LYP/ 6-311++ G(d,p)			HF/ 6-31+G (d,p)	B3LYP/ 6-311+ G(d,p)	B3LYP/ 6-311++G(d,p)			HF/ 6-31+G(d,p)	B3LYP/ 6-311+G(d,p)	B3LYP/ 6-311++G(d,p)
N1-C2	1.3136	1.3273	1.3223	1.400	C2-C1-C6	119.54	119.16	118.68	115.9	C6-N1-C2-C3	0.003	-0.0061	0.01
N1-C6	1.3245	1.3381	1.3489	1.338	N1-C2-C3	123.03	123.23	123.89	125.9	C6-N1-C2-O7	-179.99	-179.99	-179.99
C2-C3	1.3965	1.4032	1.4055	1.400	N1-C2-O7	113.58	113.12	119.51		C2-N1-C6-C5	-0.003	0.0121	-0.002
C2-O7	1.3362	1.3577	1.3529		C3-C2-O7	123.37	123.63	116.59		C2-N1-C6-C15	179.99	-179.92	180.00
C3-C4	1.3816	1.3897	1.381	1.393	C2-C3-C4	117.13	117.28	117.15	117.0	N1-C2-C3-C4	-0.0013	-0.001	0.001
C3-H12	1.0711	1.0806	1.0819		C2-C3-H12	122.16	122.12	120.00		N1-C2-C3-H12	-179.99	-179.98	-179.99
C4-C5	1.3848	1.3909	1.4003	1.375	C4-C3-H12	120.70	120.59	122.84		O7-C2-C3-C4	-180.00	179.98	179.98
C4-H13	1.0762	1.0846	1.0845	1.506	C3-C4-C5	120.15	119.90	119.71	121.6	O7-C2-C3-H12	0.0019	0.0051	0.001
C5-C6	1.3894	1.3984	1.3905	1.347	C3-C4-H13	119.58	119.70	120.06	116.3	N1-C2-O7-C8	-179.97	-179.96	0.0162
C5-H14	1.0737	1.0829	1.0829		C5-C4-H13	120.26	120.38	120.22	121.8	C3-C2-O7-C8	0.0249	0.0493	-179.98
C6-C15	1.5055	1.5062	1.5053		C4-C5-C6	117.84	118.36	118.74	119.0	C2-C3-C4-C5	-0.005	0.0023	0.001
O7-C8	1.4018	1.4219	1.4321		C4-C5-H14	121.29	121.09	120.86		C2-C3-C4-H13	180.00	-179.98	-179.99
C8-H9	1.0853	1.0885	1.0918		C6-C5-H14	120.86	120.53	120.39		H12-C3-C4-C5	179.99	179.98	179.98
C8-H10	1.0795	1.0952	1.0919		N1-C6-C5	122.28	122.03	121.81	120.7	H12-C3-C4-H13	-0.0019	-0.007	-0.001
C8-H11	1.0853	1.0953	1.0887		N1-C6-C15	115.92	116.14	116.04		C3-C4-C5-C6	0.004	0.0032	-0.003
C15-H16	1.0835	1.0914	1.0913		C5-C6-C15	121.78	121.81	122.13		C3-C4-C5-H14	180.00	-179.98	-179.99
C15-H17	1.0845	1.0932	1.0936		C2-O7-C8	120.49	118.79	117.68		H13-C4-C5-N6	179.99	179.99	179.98
C15-H18	1.0845	1.0934	1.0937		O7-C8-H9	111.40	105.68	110.97		H13-C4-C5-H14	-.0001	0.0027	-0.007
					O7-C8-H10	105.91	111.52	110.98		C4-C5-C6-N1	0.0013	-0.0107	0.004
					O7-C8-H11	111.39	111.51	105.12		C4-C5-C6-C15	-179.99	179.92	-180.00
					H9-C8-H10	109.19	109.23	108.80		H14-C5-C6-N1	-179.99	179.98	179.99
					H9-C8-H11	109.63	109.24	110.46		H14-C5-C6-C15	0.0031	-0.0829	-0.007
					H10-C8-H11	109.19	109.54	110.47		N1-C6-C15-H16	-180.00	-179.58	179.98
					C6-C15-H16	111.64	111.72	111.63		N1-C6-C15-H17	59.0432	-58.46	-59.02
					C6-C15-H17	109.86	110.13	110.28		N1-C6-C15-H18	-59.054	59.38	59.05
					C6-C15-H18	109.87	110.11	110.29		C5-C6-C15-H16	-0.0078	0.4704	0.0219
					H16-C15-H17	108.91	108.85	108.70		C5-C6-C15-H17	-120.95	121.59	120.98
					H16-C15-H18	108.51	108.79	108.7		C5-C6-C15-H18	120.94	-120.56	-120.93
					H17-C15-H18	107.51	107.06	107.08		C2-O7-C8-H9	-61.387	179.97	-60.60
										C2-C7-C8-H10	179.99	-61.429	60.50
										C2-O7-C8-H11	61.378	61.386	179.95

For numbering of atom refer Fig. 1.

[a] Value taken from Ref [33].

All the calculations such as first hyperpolarizability, HOMO–LUMO, NMR, NBO analysis were carried out by using B3LYP/6-311++G(d,p) method. It can be noted that the calculated frequencies are harmonic while the observed frequencies contain anharmonic contributions. The observed frequencies are generally lower than the calculated frequencies due to anharmonic nature of molecular vibrations. In principle, we should compare the calculated frequencies with experimental harmonic frequencies. However, as all the vibrations are more or less anharmonic, harmonic frequencies are not directly observable. Despite they can be deduced theoretically, it requires detailed knowledge of both quadratic and anharmonic force constants and is only feasible for every molecule. It should be pointed out that reproduction of observed fundamental frequencies is more desirable practically because they are directly observable in a vibrational spectrum. Therefore, comparison between the calculated and the observed vibrational spectra helps us to understand the observed spectral features. In order to improve the agreement of theoretically calculated frequencies with experimentally calculated frequencies, it is necessary to scale down the calculated frequencies by using the scale factors 0.914 and 0.87 for HF/6-311+G(d,p) and for B3LYP/6-311+G(d,p) set is scaled 0.955 and 0.93 and B3LYP/6-311++G(d,p) basis set is scaled with 0.96, 0.947 and 0.99. Hence, the vibrational frequencies theoretically calculated at HF/6-311+G(d,p), B3LYP/6-311+G(d,p) and B3LYP/6-311++G(d,p) are scaled down by using MOLVIB 7.0 version written by Tom Sundius [21-23].

Results and Discussion

Geometrical parameters

The molecular structure MMP belongs to C_1 point group symmetry. For C_1 symmetry there would not be any relevant distribution. The molecule consists of 18 atoms and expected to have 48 normal modes of vibration of the same (A) species under C_1 symmetry. The optimized structural parameters are calculated at *ab initio* (HF) 6-311+G(d,p) and DFT (B3LYP) levels with the 6-311+G(d,p)/6-311++G(d,p) basis set are listed in Table1 in accordance with the atom numbering scheme given in Fig. 1 respectively for MMP and the calculated geometrical parameters are compared with X-ray diffraction result.

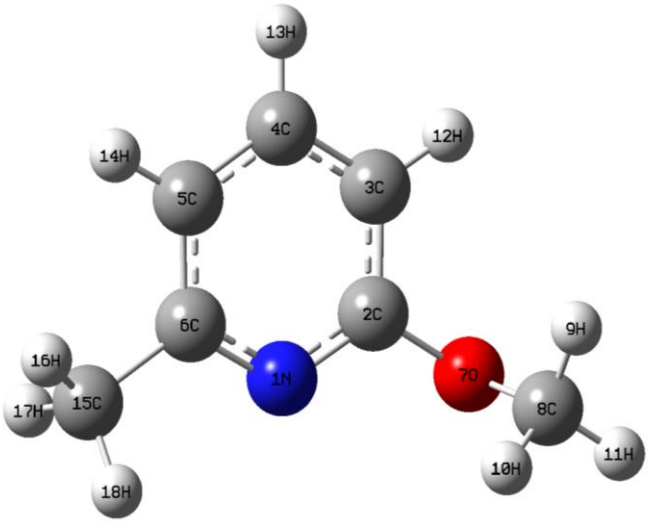

Fig 1. Molecular structure of 2-methoxy-6-methylpyridine

Detailed description of vibrational modes can be given by means of normal coordinate analysis. For this purpose, the full set of 61 standard internal coordinates (containing 13 redundancies) for MMP are presented in Table 2.

Table 2. Definition of internal coordinates of 2-methoxy-6-methylpyridine

No. (i)	Symbol	Type	Definition[a]
		Stretching	
1-3	r_i	C-H	C3-H12, C4-H13,C5-H14
4-9	r_i	C-H	C8-H9, C8-H10, C8-H11, C15-H16, C15-H17, C15-H18
10-11	Q_i	C-O	C2-O7,C8-O7
12-13	q_i	C-N	C2-N1,C6-N1
14-18	P_i	C-C	C2-C3, C3-C4, C4-C5, C5-C6, C6-C15
		In-plane bending	
19 - 24	β_i	ring	N1-C2-C3, C2-C3-C4, C3-C4-C5, C4-C5-C6, C5-C6-N1, C6-N1-C2
25 - 30	α_i	C-C-H	C2-C3-H12, C4-C3-H12, C3-C4-H13, C5-C4-H13, C4-C5-H14, C6-C5-H14
31-33	β_i	O-C-H	O7-C8-H9, O7-C8-H10, O7-C8-H11
34-36	ν_i	H-C-H	H9-C8-H10, H9-C8-H11, H10-C8-H11
37-39	β_i	C-C-H	C6-C15-H16, C6-C15-H17, C6-C15-H18
40-42	ν_i	H-C-H	H16-C15-H17, H16-C15-H18, H17-C15-H18
43	ε_i	C-C-C	C5-C6-C15
44	δ_i	N-C-C	N1-C6-C15
45	σ_i	C-C-O	C3-C2-O7
46	σ_i	N-C-O	N1-C2-O7
47	μ_i	C-O-C	C2-O7-C8
		Out-of-plane bending	
48-50	ψ_i	C-H	H12-C3-C4-C2, H13-C4-C5-C3, H14-C5-C6-C4
51	ρ_i	C-O	O7-C2-C3-N1
52	χ_i	O-C	C8-O7-C2-(C3,N1)
53	ω_i	C-C	C15-C6-N1-C5
		Torsion	
54-59	τ_i	t Ring	N1-C2-C3-C4, C2-C3-C4-C5, C3-C4-C5-C6, C4-C5-C6-N1, C5-C6-N1-C2, C6-N1-C2-C3
60	τ_i	t C-CH_3	(N1,C5)-C6-C15-(H16,H17,H18)
61	τ_i	t O-CH_3	C1-O7-C8-(H9,H10,H11)

[a] For numbering of atoms refer Fig. 1

From these, a non-redundant set of local symmetry coordinates are constructed by suitable linear combinations of internal coordinates following the recommendations of Pulay and Fogarasi [24] which are presented in Tables 3, respectively for MMP. The experimentally and theoretically calculated IR, Raman frequencies are presented in Table 4 respectively for MMP. The FT-IR and FT-Raman spectra of the MMP are shown in Fig. 2-3.

C-H vibrations

The hetero aromatic structure shows the presence of C-H stretching vibration in the region 3100-3000 cm^{-1} which is the characteristic region for the identification of such C-H stretching vibrations. These vibrations are not found to be affected due to the nature and position of the substituents. In the present investigation, the C–H vibrations are observed at 3151 cm^{-1} in the FTIR spectrum and at 3176, 3157, 3152 cm^{-1} in the FT Raman spectrum for MMP, respectively.

Table 3. Definition of local symmetry coordinates of 2-methoxy-6-methylpyridine

No. (i)	Type	Definition[b]
1-3	C H	r_1, r_2, r_3
4,5	CH_3 ss	$(r_4 + r_5 + r_6)/\sqrt{3}$, $(r_7 + r_8 + r_9)/\sqrt{3}$
6,7	CH_3 ass	$(2r_4 + r_5 + r_6)/\sqrt{6}$, $(2r_7 + r_8 + r_9)/\sqrt{6}$
8,9	CH_3 ops	$(r_5 - r_6)/\sqrt{6}$,$(r_8 - r_9)/\sqrt{6}$
10,11	C O	Q_{10},Q_{11}
12-13	C N	q_7, q_8
14-18	CC	P_{14},P_{15},P_{16},P_{17},P_{18}
19	R trigd	$(\beta_{19} - \beta_{20} + \beta_{21} - \beta_{22} + \beta_{23} - \beta_{24})/\sqrt{6}$
20	R symd	$(-\beta_{19} - \beta_{20} + 2\beta_{21} - \beta_{22} - \beta_{23} - 2\beta_{24})/\sqrt{12}$
21	R asymd	$(\beta_{19} - \beta_{20} + \beta_{22} - \beta_{23})/\sqrt{2}$
22-24	b C H	$(\alpha_{25} - \alpha_{26})/\sqrt{2}$, $(\alpha_{27} - \alpha_{28})/\sqrt{2}$,$(\alpha_{29} - \alpha_{30})/\sqrt{2}$
25,26	CH_3 sb	$(-\beta_{31} - \beta_{32} - \beta_{33} + \nu_{34} + \nu_{35} + \nu_{36})/\sqrt{2}$ $(-\beta_{37} - \beta_{38} - \beta_{39} + \nu_{40} + \nu_{41} + \nu_{42})/\sqrt{2}$
27,28	CH_3 ipb	$(2\nu_{34} - \nu_{35} - \nu_{36})/\sqrt{6}$,$(2\nu_{40} - \nu_{41} - \nu_{42})/\sqrt{6}$
29,30	CH_3 opb	$(-\nu_{34} + \nu_{35})/\sqrt{2}$ $(-\nu_{40} + \nu_{41})/\sqrt{2}$
31,32	CH_3 ipr	$(-\beta_{31} - \beta_{32} + 2\beta_{33})/\sqrt{6}$,$(-\beta_{37} - \beta_{38} + 2\beta_{39})/\sqrt{6}$
33,34	CH_3 opr	$(-\beta_{32} + \beta_{33})/\sqrt{2}$,$(-\beta_{38} + \beta_{39})/\sqrt{2}$
35	b C C	$(\pi_{43} - \delta_{44})/\sqrt{2}$
36	b C O	$(\sigma_{43} - \sigma_{44})/\sqrt{2}$
37	b O C	μ_{45}
38-40	ω C H	ψ_{48},ψ_{49},ψ_{50}
41	ω C O	ρ_{51}
42	ω OC	χ_{52}
43	ω CC	ω_{53}
44	Ring trigd	$(\tau_{54} - \tau_{55} + \tau_{56} - \tau_{57} + \tau_{58} - \tau_{59})/\sqrt{6}$
45	Ring symd	$(\tau_{54} - \tau_{56} + \tau_{57} - \tau_{59})/\sqrt{2}$
46	Ring asymd	$(-\tau_{54} + 2\tau_{55} - \tau_{56} - \tau_{57} + 2\tau_{58} - \tau_{59})/\sqrt{12}$
47	t C-CH_3	τ_{60}
48	t O-CH_3	τ_{61}

[b] The internal coordinates used here are defined in Table 2.

The C-H in-plane-bending vibrations usually occur in the region 1390-990 cm^{-1} and are very useful for characterization purposes. Substitution patterns on the ring can be judged from the out-of-plane bending vibrations occur in the region 900-675 cm^{-1} and these bands are highly informative [25]. Therefore, the IR peaks observed at 1245, 1238 cm^{-1} and at 1222 cm^{-1} in Raman spectrum for MMP have been assigned to, C-H in-plane-bending vibrations. The C-H out-of-plane bending vibrations are observed at 633,610 cm^{-1} in IR and in Raman 623 $cm^{-1}$for MMP.

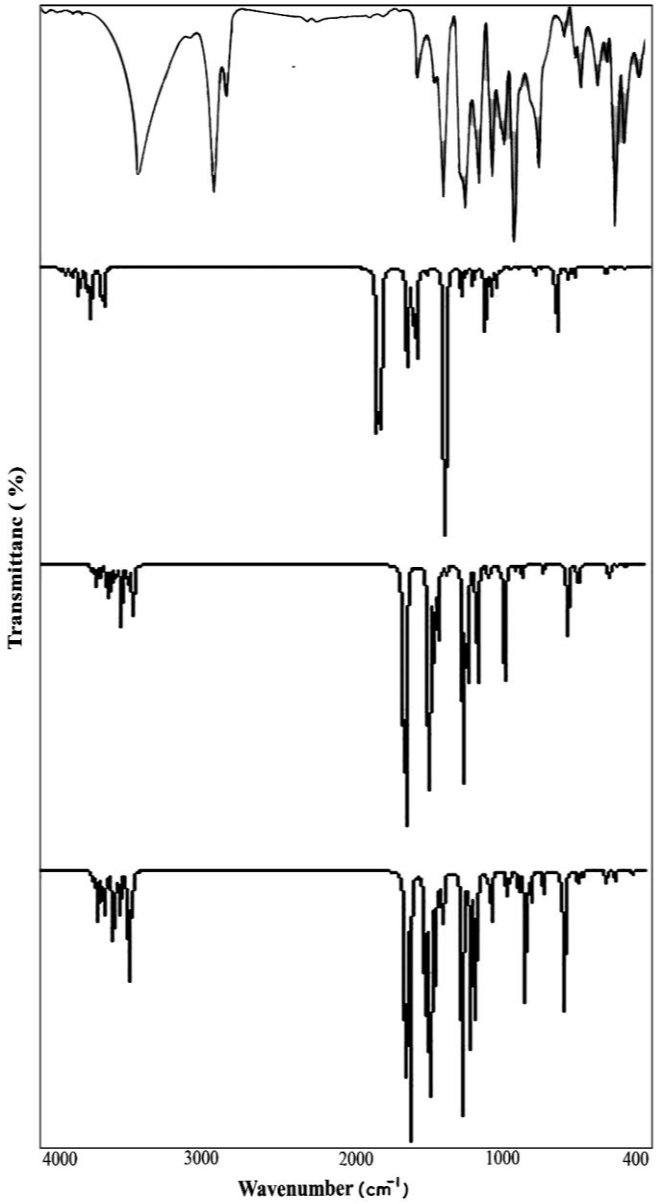

Fig 2. Observed and calculated IR spectrum of 2-methoxy-6-methylpyridine (a) Observed (b) HF/6-311+G(d,p) (c) B3LYP/6-311+G(d,p) (d) B3LYP/6-311++G(d,p)

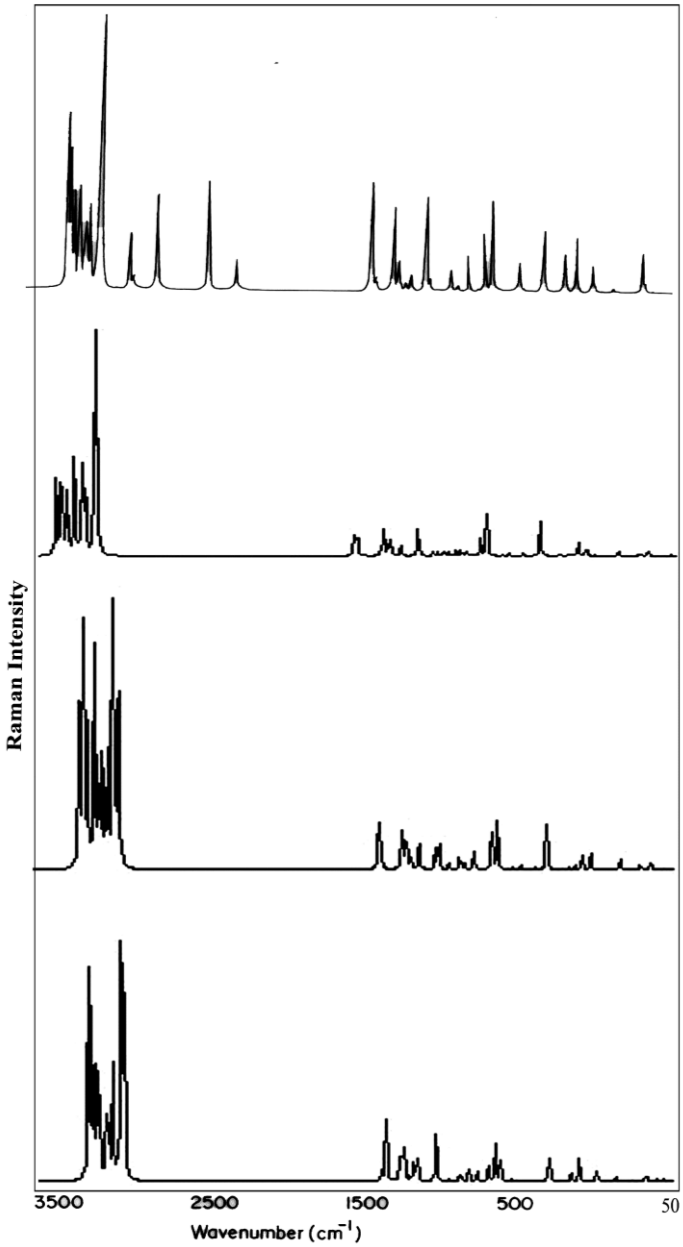

Fig 3. Observed and calculated Raman spectrum of 2-methoxy-6-methylpyridine
(a) Observed,(b)HF/6-311+G(d,p),(c)B3LYP/6-311+G(d,p) (b) B3LYP/6-311++G(d,p).

C-C vibrations

The C-C heteroaromatic stretching vibrations are occurring near 1650-1400 cm^{-1} are good group vibrations [25]. With heavy substituents, the bonds tend to shift to somewhat lower wavenumbers and greater the number of substituents on the ring, broader the absorption regions. As predicted in the earlier references, in the present investigation, the C–C stretching vibrations observed at 1753, 1612 cm^{-1} in FT-IR and 1744, 1601, 1503 cm^{-1} in FT-Raman for MMP are assigned to C–C stretching vibrations are confirmed by their TED values. Most of the ring vibrational modes are affected by the substitutions in the hetero aromatic ring of MMP. In the present study, the bands are observed at 888 cm^{-1} in the FTIR for MMP has been designated to ring in-plane bending modes by careful consideration of their quantitative descriptions. The ring out-of-plane bending modes of MMP are also listed in Tables 4, respectively.

Table 4. The observed (FTIR and FT-Raman) and calculated (unscaled and scaled) fundamental harmonic frequencies (cm^{-1}), of 2-methoxy-6-methylpyridine are analysed based on SQM force field calculation using HF/6-311+G(d,p), B3LYP/6-311+G(d,p) and B3LYP/6-311++G(d,p) method and basis set calculations

Observed frequencies		Calculated frequency (cm^{-1}) with HF/6-311+G(d,p)		Calculated frequency (cm^{-1}) with B3LYP/ 6-311+G(d,p)		Calculated frequency (cm^{-1}) with B3LYP/ 6-311++G(d,p)		Assignments (TED %)
FTIR	FT-Raman	Unscaled	Scaled	Unscaled	Scaled	Unscaled	Scaled	
-	3176(s)	3408	3204	3215	3173	3206	3174	υCH(99)
-	3157(ms)	3379	3190	3199	3154	3191	3159	υCH(98)
3151(vs)	3152(s)	3350	3175	3189	3151	3170	3154	υCH(97)
-	2998(vs)	3311	3100	3176	3009	3141	3000	CH3ss(62), CH3ops(23), CH3ipb(14)
-	2991(vs)	3282	3087	3166	2994	3112	2993	CH3ss(63), CH3ops(21), CH3ipb(15)
2986(s)	2985(ms)	3261	3068	3091	2990	3105	2989	CH3ips(60), CH3ss(22), CH3ops(16)
2971(vw)	2972(ms)	3250	3051	3065	2979	3085	2977	CH3ips(61), CH3ss(24), CH3ops(12)
2490(w)	2491(s)	3212	2989	3034	2688	3068	2495	CH3ops(58), CH3ips(20), CH3ss(11)
2481(vw)	2380(s)	3205	2878	3006	2679	2467	2383	CH3ops, (57) CH3ips(18), CH3ss(12)
1753(w)	-	1892	1790	1828	1749	1733	1755	υCC(64), CH3ipb(17), CH3sb(14)
-	1744(w)	1870	1810	1817	1789	1718	1747	υCC(56), CH3ipb(19), CH3sb(11
1612(w)	-	1843	1790	1706	1689	1678	1615	υCC(65), CH3sb(16), υCO(11)
-	1601(w)	1795	1689	1699	1680	1656	1607	υCC(66), CH3sb(17), υCO(9)
-	1503(w)	1730	1650	1686	1667	1645	1507	υCC(63), υCO(21), υCN(12)
1491(ms)	1493(vw)	1722	1630	1673	1589	1579	1494	CH3ipb(68), υCC(16), υCN(9)
1480(ms)	1482(w)	1707	1598	1657	1570	1564	1487	CH3ipb(69), υCC(15), CH3ips(10)
1465(ms)	1467(w)	1699	1688	1647	1516	1547	1466	CH3sb(57), υCC(19), CH3ips(14)
1412(vw)	1410(w)	1678	1666	1634	1507	1539	1416	CH3sb(55), υCC(15), bCH(11)
1391(w)	-	1642	1631	1609	1490	1511	1397	υCN(59), υCC(18), bCH(14)
-	1386(w)	1613	1601	1589	1473	1467	1388	υCN(61),υCO(17), υCC(12)
1292(w)	-	1599	1578	1572	1469	1454	1295	υCO(53), υCN(21), υCC(16)
1288(w)	1289(w)	1578	1567	1563	1454	1445	1291	υCO(56), υCN(22), υCC(14)
1245(s)	-	1562	1529	1556	1440	1420	1244	bCH(58), CH3opb(22), υCC(9)
1238(s)	-	1552	1512	1534	1423	1412	1242	bCH(59), CH3opb(23), υCC(11)
-	1222(w)	1538	1501	1523	1412	1401	1227	bCH(51), CH3opr(24), CH3opb(15)
1190(ms)	1192(w)	1519	1489	1501	1405	1389	1197	CH3opb(50), bCC(25), CH3opr(14)
1185(vw)	1184(ms)	1511	1478	1467	1389	1372	1189	CH3opb(52), Rtrigd(23), CH3opr(18)
1147(w)	1148(w)	1501	1468	1456	1378	1357	1150	CH3opr(57), Rsymd(18), CH3opb(13)
1135(s)	1137(vw)	1489	1473	1378	1363	1347	1138	CH3opr(55), Rasymd(25), CH3ipr(12)
986(vw)	985(w)	1472	1465	1367	1354	1334	1123	CH3ipr(53), bCO(21), bCC(18)
971(w)	972(w)	1465	1453	1352	1334	1321	977	CH3ipr(52), bCO(20) bCH(15)
888(w)	-	1454	1423	1329	1323	1301	898	bCC(51), CH3opr(19), CH3ipr(12)
-	878(w)	1430	1412	1312	1306	1298	884	Rtrigd(50), CH3ipr(17), bCO(13)
-	865(w)	1399	1383	1301	1299	1278	873	Rsymd(45), CH3ipr(22), bCO(17)
852(w)	852(vw)	1109	1006	999	991	890	865	Rasymd(49), ωCH(24), CH3ipr(14)
-	763(w)	1089	995	987	860	827	769	bCO(48), ωCH(26), Rtrigd(13)
-	752(w)	1067	982	915	851	815	758	bCO(51), ωCH(19), Rsymd11)
633(vw)	-	1054	970	882	878	780	639	ωCH(49), ωCC(27), Rasymd(17)
-	623(w)	1023	956	943	822	752	625	ωCH(46), tRtrigd(27), ωCO(19)
610(w)	-	1003	934	928	708	739	619	ωCH(44), tRsymd(23), ωCO(15)
-	600(s)	998	921	912	689	653	607	ωCC(43), tRasymd(21), ωCH(17)
505(s)	-	945	905	871	700	566	505	tRtrigd(42), ωCO(22), ωCH(18)
-	499(vw)	888	873	834	678	545	510	tRsymd(48), ωCO(21), ωCH(12)
482(vw)	-	856	745	736	583	506	487	tRasymd(55)
386(w)	-	823	756	722	688	602	395	ωCO(65)
312(w)	-	706	601	579	510	464	319	ωCO(73)
-	152(w)	606	534	512	467	410	162	tCCH3(71)
-	99(vw)	560	445	364	294	191	107	tOCH3(67)

Abbreviations

ν- stretching; b - in-plane bending; ω - out-of-plane bending; asymd - asymmetric; symd - symmetric; t - torsion; trig - trigonal; w - weak; vw - very week; vs - very strong; s - strong; ms - medium strong; ss - symmetric stretching; ass - asymmetric stretching; ips - in-plane stretchingj; ops - out-of-plane stretching; sb - symmetric bending; ipr - in-plane rocking; opr - out-of-plane rocking; opb - out-of-plane bending.

C-N vibrations

In hetero aromatic compounds, the C-N stretching vibration usually lies in the region 1400 - 1200 cm^{-1}. The identification of C-N stretching frequencies is a rather difficult task. Since the mixing of vibrations is possible in this region [25]. In this study, the C–N stretching vibrations of MMP are found at 1391 cm^{-1} in the FTIR spectrum and at 1386 cm^{-1} in the FT-Raman spectrum. The C–N bending vibrations and deformations are in close agreement with literature value and also supported the TED values.

C–O vibrations

The interaction of the carbonyl group with a hydrogen donor group does not produce drastic and characteristic changes in the frequency of the C=O stretch as does by O–H stretch. A great deal of structural information can be derived from the exact position of the carbonyl stretching absorption peak. *Sambathkumar et al*.[26] identified the C=O stretching mode at 1645 and 1614 cm^{-1}. On referring to the above findings and on the basis of the results of the normal coordinate analysis, the present investigation, the C–O stretching vibrations have been found at 1292, 1288 cm^{-1} in IR and 1289 cm^{-1} in Raman for MMP. The C–O in-plane and out-of-plane bending vibrations level also have been identified and presented in Table 4 for MMP.

CH_3 group vibrations

The investigated molecule under consideration possesses CH_3 groups in sixth and seventh position of MMP. For the assignments of CH_3 group frequencies one can expected that nine fundamentals can be associated to each CH_3 group, namely three stretching, three bending, two rocking modes and a single torsional mode describe the motion of methyl group. The above modes are defined in Table 4. The CH_3 symmetric stretching frequency is identified at 2998, 2991 cm^{-1} in the FT-Raman spectrum for MMP. The CH_3 in-plane stretching vibrations are identified at 2986, 2971 cm^{-1} in the FTIR spectrum and at 2985, 2972 cm^{-1} in the FT-Raman spectrum for MMP. The CH_3 symmetric bending and CH_3 in-plane bending frequencies are attributed at 1465, 1412 cm^{-1} and 1491, 1480 cm^{-1} in the FTIR spectrum and at 1467, 1410 cm^{-1} and 1493, 1482 cm^{-1} in the FT Raman spectrum for MMP. These assignments are supported by literature [25]. The in-plane rocking and out-of-plane rocking modes of CH_3 group are found at 986, 971 cm^{-1} and 1147, 1135 cm^{-1} in the FTIR spectrum and at 985, 972 cm^{-1} and 1148, 1137 cm^{-1} in the FT-Raman spectrum for MMP. The bands obtained at 2490, 2481 cm^{-1} and 1190, 1185 cm^{-1} in the FTIR spectrum and at 2491, 2380 cm^{-1} and 1192, 1184 cm^{-1} in the FT-Raman spectrum for MMP are assigned to CH_3 out-of-plane stretching and CH_3 out-of-plane bending modes, respectively. The assignment of the bands at 152, 99 cm^{-1} in the FT-Raman spectrum, respectively for MMP attributed to methyl twisting mode.

Prediction of Non-Linear Optical Properties

The first hyperpolarizability (β_0) of this novel molecular system and the related properties (β_0,α_0) of MMPare calculated using the HF/6-311+G(d,p) and B3LYP/6-311++G(d,p) basis set, based on the finite field approach. In the presence of an applied electric field, the energy of a system is a function of the electric field. The first hyperpolarizability is a third-rank tensor that can be described by a $3 \times 3 \times 3$ matrix. The 27 components of the 3D matrix can be reduced to 10 components due to the Kleinman symmetry [26]. It can be given in the lower tetrahedral. The components of β are defined as the coefficients in the Taylor series expansion of the energy in the external electric field. When the external electric field is weak and homogenous, this expansion becomes:

$$E= E_0 - \mu_\alpha F_\alpha - 1/2\alpha_{\alpha\beta}F_\alpha F_\beta - 1/6\beta_\alpha\beta_\gamma F_\alpha F_\beta F_\gamma + ...$$

where E_0 is the energy of the unperturbed molecules, F_α the field at the origin and μ_α, $\alpha_{\alpha\beta}$ and $\beta_\alpha\beta_\gamma$ are the components of dipole moment, polarizability and the first hyperpolarizabilities, respectively. The total static dipole moment μ, the mean polarizability α_0 and the mean first hyperpolarizability β_0, using the x, y, z components they are defined as

$$\mu = (\mu_x^2+\mu_y^2+\mu_z^2)^{1/2}$$

$$\alpha_0 = (\alpha_{xx}+\alpha_{yy}+\alpha_{zz})/3$$

$$\alpha = 2^{-1/2}[(\alpha_{xx}-\alpha_{yy})^2 + (\alpha_{yy}-\alpha_{zz})^2 + (\alpha_{zz}-\alpha_{xx})^2 + 6\alpha_{xx}^2)^{1/2}$$

$$\beta_0 = (\beta_x^2+\beta_y^2+\beta_z^2)^{1/2}$$

$$\beta_{vec} = 3/5[(\beta_x^2+\beta_y^2+\beta_z^2)^{1/2}]$$

where

$$\beta_x = \beta_{xxx} + \beta_{xyy} + \beta_{xzz}$$

$$\beta_y = \beta_{yyy} + \beta_{yxx} + \beta_{yzz}$$

$$\beta_z = \beta_{zzz} + \beta_{zxx} + \beta_{zyy}$$

The β_0 components of GAUSSIAN 09W program package output are reported in atomic units andtherefore the calculated values are converted into e.s.u. units (1 a.u. = 8.3693×10^{-33} e.s.u.). The calculated value of hyperpolarizability and polarizability of MMPare tabulated in Table 5.

Table 5. Nonlinear optical properties of 2-methoxy-6-methylpyridinecalculated at HF/6-311++G(d,p) with B3LYP/6-311+G(d,p) and 6-311++G(d,p) method and basis set calculations

NLO behaviour	HF/ 6-311+G(d,p)	B3LYP/ 6-311+G(d,p)	B3LYP/ 6-311++G(d,p)
Dipole moment (μ)	1.1472 Debye	1.0867 Debye	0.3043Debye
Mean polarizability (α)	0.7313×10^{-30} esu	0.8117×10^{-30} esu	0.8095×10^{-30} esu
Anisotropy of the polarizabilty (Δ_α)	1.4354×10^{-30} esu	1.9302×10^{-30} esu	1.8394×10^{-30} esu
First hyperpolarizability (β)	1.8399×10^{-30} esu	1.3284×10^{-30} esu	2.2406×10^{-30} esu
Vector-first hyperpolarizability (β_{vec})	1.1039×10^{-30} esu	0.7970×10^{-30} esu	1.3443×10^{-30} esu

We can conclude that the title molecules are an attractive object for future studies of non-linear optical properties.

HOMO-LUMO Analysis

This electronic absorption corresponds to the transition from the ground to the first excited state and is mainly described by one electron excitation from the highest occupied molecular orbital (HOMO) to the lowest unoccupied molecular orbital (LUMO) [25,26]. Many organic molecule, containing conjugated π electrons are characterized by large values of molecular first hyper polarizabilities, are analyzed by means of vibrational spectroscopy. In most of the cases, even in the absence of inversion symmetry, the strongest band in the Raman spectrum is weak in the IR spectrum and vice-versa. But the intra molecular charge from the donor to acceptor group through a single-double bond conjugated path can induce large variations of both the molecular dipole moment and the molecular polarizability, making IR and Raman activity strong at the same time. The analysis of the wave function indicates that the electron absorption corresponds to the transition from the ground to the first

excited state and is mainly described by one-electron excitation from the highest occupied molecular orbital (HOMO) to the lowest unoccupied orbital (LUMO). In MMP the HOMO is located over heterocyclic ring and the HOMO-LUMO transition implies an electron density transfer to the CH_3, group from heterocyclic ring and oxygen atom, whereas in MMP the HOMO is located over heterocyclic ring, especially on amino and oxygen atom, and the HOMO-LUMO transition implies an electron density transfer to the heterocyclic ring from amino group and oxygen atom. Moreover, the composition of HOMO and LUMO for MMP are shown in Fig. 4, respectively.

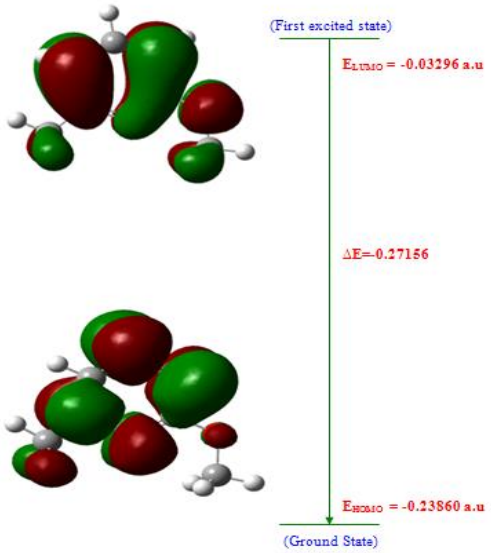

Fig 4. HOMO-LUMO Plot of 2-methoxy-6-methylpyridine

The HOMO-LUMO energy gap of MMP were calculated at B3LYP/6-311++G(d,p) level, which reveals that the energy gap reflects the chemical activity of the molecules. The LUMO as an electron acceptor (EA) represents the ability to obtain an electron donor (ED) and HOMO represents ability to donate an electron donor (ED). The ED groups to the efficient EA groups through π-conjugated path. The strong charge transfer interaction through π-conjugated bridge results in substantial ground state Donor-Acceptor (DA) mixing and the appearance of a charge transfer band in the electron absorption spectrum. The HOMO-LUMO energy gap explains the fact that eventual charge transfer interaction is taking place within the investigated molecules.

Global and local reactivity descriptors

Based on density functional descriptors global chemical reactivity descriptors of compounds such as hardness, chemical potential, softness, electronegativity and electrophilicity index as well as local reactivity have been defined [25-27]. Pauling introduced the concept of electronegativity as the power of an atom in a compound to attract electrons to it. Hardness (η), chemical potential (μ) and electronegativity (χ) and softness are defined follows.

$\eta = \frac{1}{2}(\partial^2 E/\partial N^2)_{V(r)}$

$= \frac{1}{2}(\partial\mu/\partial N)_{V(r)}$

$\mu = (\partial E/\partial N)_{V(r)}$

$\chi = -\mu = -(\partial E/\partial N)_{V(r)}$

where E and V(r) are electronic energy and external potential of an N-electron system respectively. Softness is a property of compound that measures the extent of chemical reactivity. It is the reciprocal of hardness.

$S = 1/\eta$

Using Koopman's theorem for closed-shell compounds, η, μ and χ can be defined as

$\eta = (I-A)/2$

$\mu = -(I+A)/2$

$\chi = (I+A)/2$

where A and I are the ionization potential and electron affinity of the compounds respectively. Electron affinity refers to the capability of a ligand to accept precisely one electron from a donor. However in many kinds of bonding viz. covalent hydrogen bonding, partial charge transfer takes places. Recently Parr *et al.* [28] have defined a new descriptor to quantity the global electrophilic power of the compound as electrophilicity index (ω), which defines a quantitative classification of the global electrophilic nature of a compound have proposed electrophilicity index (ω) as a measure of energy lowering due to maximal electron flow between donor and acceptor. They define electrophilicity index (ω) as

$\omega = \mu^2/2\eta$

The usefulness of this new reactivity quantity has been recently demonstrated in understanding the toxicity of various pollutants in terms of their reactivity and site selectivity [29-31]. The calculated value of electrophilicity index describes the biological activity for MMP respectively. All the calculated values of HOMO-LUMO, energy gap, ionization potential, Electron affinity, hardness, potential, softness and electrophilicity index are shown in Table 6.

Table 6. HOMO-LUMO energy gap and related molecular properties of 2-methoxy-6-methylpyridine.

Molecular Properties	B3LYP/6-311++G(d,p)
HOMO	-0.23860
LUMO	-0.03296
Energy gap	0.20564
Ionisation Potential (I)	0.23860
Electron affinity(A)	0.03296
Global softness(s)	9.7257
Global Hardness (η)	0.10282
Chemical potential (μ)	-0.135578
Global Electrophilicity (ω)	0.08962

NBO Analysis

The NBO analysis is carried out by examining all possible interactions between 'filled' (donor) Lewis-type NBOs and 'empty' (acceptor) non-Lewis NBOs, and estimating their energetic important by 2nd order perturbation theory. Since these interactions lead to loss of occupancy from the localized NBOs of the idealized Lewis structure into the empty non-Lewis orbitals, they are referred to as delocalization corrections to the zeroth-order natural Lewis structure. For each donor NBO (i) and acceptor NBO (j) with delocalization $i \rightarrow j$ is estimated as

$$E^{(2)} = \Delta E_{ij} = q_i \frac{F(i,j)^2}{\varepsilon_j - \varepsilon_i}$$

where q_i is the donor orbital occupancy ε_j and ε_i are diagonal elements orbital energies and F(i, j) is the off diagonal NBO Fock matrix element. The larger $E^{(2)}$ value, the more intensive is the interaction between electron donors and acceptors, i.e., the more donation tendency from electron donors to electron acceptors and the greater the extent of conjugation of the whole system.

Table 7. Second-order perturbation theory analysis of Fock matrix in NBO basis of 2-methoxy-6-methylpyridine using DFT/B3LYP/6-311++G(d,p)basis set

Donor(i)	Type	ED/e	Acceptor (j)	Type	ED/e	$E^{(2)a}$(kJ/mol)	E(j)-E(i)[b] (a.u)	F(i,j)[c](a.u)
N1-C2	π	0.8598	C3-C4	π^*	0.2058	26.2336	0.32	0.057
N1-C2	π		C5-C6	π^*		55.2288	0.36	0.061
C3-C4	σ	0.9881	C2-O7	σ^*	0.0077	8.2843	0.99	0.0556
C3-C4	π	0.8305	N1-C2	π^*	0.1616	58.9944	0.26	0.078
C3-H12	σ	0.9892	N1-C2	σ^*	0.0067	9.5395	1.06	0.062
C5-C6	π	0.8113	N1-C2	π^*	0.1591	36.6936	0.26	0.060
C5-C6	π		C3-C4	π^*		50.2916	0.28	0.074
C5-H14	σ	0.9896	N1-C6	σ^*	0.0067	10.5018	1.07	0.065
C15-H16	σ	0.9925	N1-C6	σ^*	0.0018	8.7864	1.05	0.059
N1	LP(1)	0.9961	C2-C3	σ^*	0.0032	18.9953	0.87	0.081
N1	LP(1)		C2-O7	σ^*		13.7653	0.61	0.057
N1	LP(1)		C5-C6	σ^*		20.8363	0.89	0.085
O7	LP(1)	0.9998	N1-C2	π^*	0.0027	10.2926	0.58	0.053
O7	LP(2)	0.9672	N1-C2	σ^*	0.0012	17.9493	0.82	0.076
O7	LP(2)		C2-C3	σ^*		10.6692	0.85	0.059
O7	LP(2)		C8-H9	σ^*		10.8784	0.71	0.055
O7	LP(2)		C8-H10	σ^*		11.5060	0.72	0.057
N1-C2	π^*		C3-C4	π^*		362.9620	0.02	0.085
N1-C2	π^*		C5-C6	π^*		240.1197	0.03	0.081

[a] $E^{(2)}$ means energy of hyper conjugative interaction (stabilization energy).
[b] Energy difference between donor and acceptor i and j NBO orbitals.
[c] F (i, j) is the Fork matrix element between i and j NBO orbitals.

DFT (B3LYP/6-311++G(d,p)) level computation is used to investigate the various second-order interactions between the filled orbitals of one subsystem and vacant orbitals of another subsystem, which is a measure of the delocalization or hyper-conjugation [27]. NBOs are localized electron pair orbitals for bonding pairs and lone pairs. The hybridization of the atoms and the weight of each atom in each localized electron pair bond are calculated in the idealized Lewis structure. A normal Lewis structure would not leave any antibonding orbitals, so the presence of antibonding orbitals shows deviations from normal Lewis structures. Anti bonding localized orbitals are called non-Lewis NBOs. In order to study the small deviations from idealized Lewis structure, the Donor–Acceptor interaction approach is adopted. In MMP, π(C5-C6) → π*(C3-C4) interaction is seen to give a strong stabilization 50.29 kJ/mol. This strong stabilization denotes the larger delocalization. The interesting interactions in MMPmolecule are LP1N1, LP2O7 with that of antibonding C5-C6, N1-C2 and N1-C2, C5-C6. These two interactions result the stabilization energy of 20.83, 17.94 kJ/mol respectively. This highest interaction around the ring can induce the large bioactivity in the molecule. This shows that the lone pair orbital participates in electron donation in the molecule. The calculated values of $E^{(2)}$ are shown in Tables 7 for MMP respectively.

^{13}C and ^{1}H NMR Spectral Analysis

The molecular structure of MMPis optimized by using B3LYP method with 6-31++G(d,p)basis set. Then, GIAO ^{13}C calculations of the title compound are calculated and compared with experimental values [32] are shown in Table 8 Relative chemical shifts are then estimated by using the corresponding TMS shielding calculated in advance at the theoretical level as reference. Changes in energy needed to flip protons are called chemical shifts. The location of chemical shifts (peaks) on a NMR spectrum are measured from a reference point that the hydrogens in a standard reference compound —$(CH_3)_4S_i$ or tetramethylsilane (TMS)—produce.

Table 8. The calculated shifts of carbon and hydrogen atoms of 2-methoxy-6-methylpyridine using B3LYP/6-311++G(d,p) GIAO method

Atom position	Isotropic chemical shielding tensor (σ) (ppm)	Chemical shifts (δ) (ppm)		
		Theoretical	Expt[a]	Δ
N1	-87.7738	346.174		
C2	0.7506	181.715	163.67	-18.045
C3	63.7983	166.97	107.09	-59.88
C4	39.1534	143.312	138.67	-4.642
C5	56.7176	125.748	115.63	-10.118
C6	15.4953	118.667	156.29	37.623
O7	215.2153	104.785		
C8	122.8899	59.575	53.18	-6.395
H9	29.1692	2.7129		
H10	28.6847	3.1874		
H11	28.6085	3.2736		
H12	25.2823	6.5998	7.432	0.8322
H13	24.3609	7.5212	6.697	-0.8542
H14	24.9880	6.8914	6.697	-0.1944
C15	159.3824	23.0832	24.16	1.0768
H16	30.1565	1.7256		
H17	29.8371	2.045		
H18	30.1013	1.7808		

[a] Taken from Ref [34] and Δ (δ_{exp}-δ_{the}); difference between respective chemical shifts.

The amount of energy necessary to flip protons in TMS is assigned the arbitrary value of zero δ. Chemical shifts are measured in parts per million magnetic field strength difference (δ-scale), relative to TMS. The experimental values of MMP for ^{1}H and ^{13}C isotropic chemical shielding for TMS were 7.43 ppm and 156.29, 163.67 ppm, respectively [32]. All the calculations are performed using GAUSSVIEW molecular visualization program and Gaussian 09W program package. The result shows that the range ^{13}C NMR chemical shift of the typical organic compound usually is > 100 ppm [32], the accuracy ensures reliable interpretation of spectroscopic

parameters. In practice, it is easier to fix the radio wave frequency and vary the applied magnetic field than it is to vary the radio wave frequency. The magnetic field "felt" by a hydrogen atom is composed of both applied and induced fields. The induced field is a field created by the electrons in the bond to the hydrogen and the electrons in nearby π bonds. When the two fields reinforce each other, a smaller applied field is required to flip the proton. In this situation, a proton is said to be deshielded. When the applied and induced fields oppose each other, a stronger field must be applied to flip the proton. In this state, the proton is shielded. Electronegative atoms such as O_2, NH_2 and halogens deshield hydrogens. The extent of deshielding is proportional to the electronegativity of the heteroatom and its proximity to the hydrogen. Electrons have an heterocyclic ring, double bonded atoms, and triple bonded atoms deshield attached hydrogens. These bromine, amino and oxygen atoms show electronegative property, so that the theoretical chemical shift of C_2, C_3, C_4, C_5 and C_6 seems to be 181.715, 166.97, 143.312, 125.748 and 118.667 ppm for MMP. The chemical shift of C_2 is greater than the other carbon values. This increase in chemical shift is due to the substitution of more electronegative oxygen and amino atoms in the heterocyclic ring. The presence of electronegative atom attracts all electron clouds of carbon atoms towards the oxygen and amino atoms, which leads to deshielding of carbon atom and net result in increase in chemical shift value.

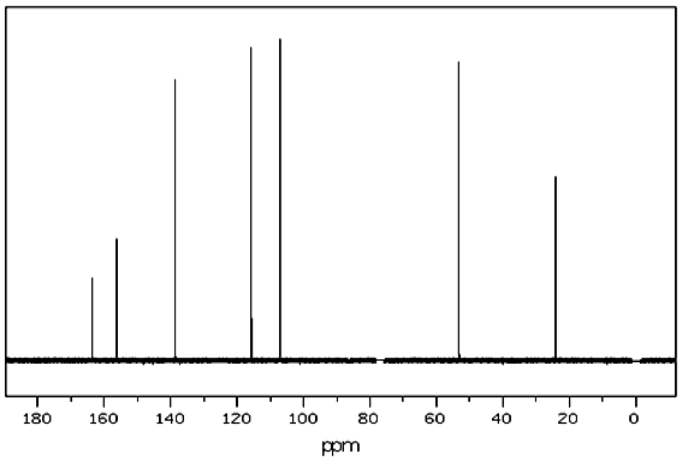

Fig 5. Observed ^{13}C NMR spectrum of 2-methoxy-6-methylpyridine

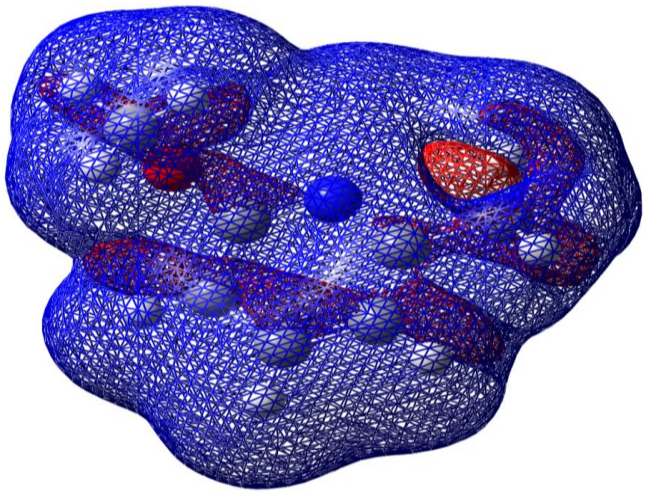

Fig 6. NMR shielding surface of 2-methoxy-6-methylpyridine

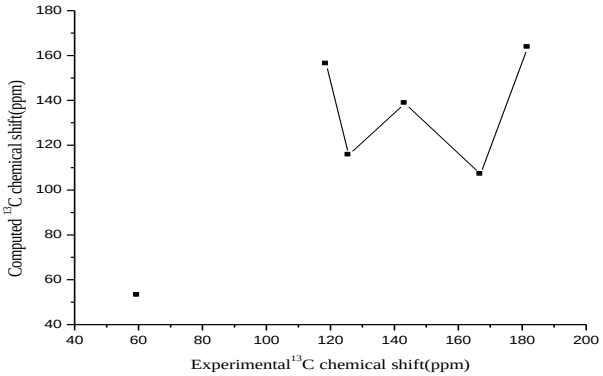

Fig 7. Computed and experimental values of 2-methoxy-6-methylpyridine

The NMR shielding surfaces of C_4 is shown in this work the chemical shift (δ) for carbon atoms presented in the MMP in gas phase has been studied and experimental ^{13}C, ^{1}H-NMR isotropic shielding of carbon and Hydrogen atom are shown in Fig. 5. In the NMR shielding surfaces, the blue region represents shielding and red region represents de-shielding are shown in Fig. 6 The relationship between the experimental chemical shift and computed GIAO/B3LYP/6-31++G(d,p) levels for ^{13}C are shown in Figs. 7 for MMP, respectively.

Conclusion

The optimized geometries, harmonic vibrational wave numbers and intensities of vibrational bands of 2-methoxy-6-methyl pyridine have been determined using HF/6-311+G(d,p), DFT/6-311+G(d,p) and DFT/6-311++G(d,p) methods and basis sets. This DFT based quantum mechanical approach provides the most reliable theoretical information on the vibrational properties of the molecules. The scaled B3LYP/6-311++G(d,p) results are the best over the other basis set. The influence of CH_3 group and the electron withdrawing nature of O atom in the MMP were also discussed. NMR (^{1}H and ^{13}C) spectral studies were carried out. The normal modes of MMP have been studied by FTIR and FT-Raman spectroscopies. The HOMO-LUMO energy gap of MMP calculated at the HF/311+G(d,p), DFT/6-311+G(d,p) and DFT/6-311++G(d,p) level reveals that the energy gap reflect the chemical activity of the molecule. Lower in the HOMO-LUMO energy gap explains the eventual charge transfer interactions taking place within the molecule. NBO analysis has been performed on MMP molecule in order to elucidate intermolecular hydrogen bonding, charge transfer (CT), rehybridization, delocalization of electron density and cooperative effect due to L(N1) $\rightarrow$ σ*(C-C) for MMP. The assignments of most of the fundamentals provided in the present investigations are believed to be unambiguous.

References

[1] T.L. Gilchrist, Heterocyclic chemistry, Addison Wesley Longman (1997).

[2] M. Okamato, K. Takahashi, T. Doi, Y. Takimoto, Anal. Chem., 69 (1997) 2919.

[3] Z. Dega-Szafran, A. Kania, B. Nowak-Wyadra, M. Szafran, J. Mol. Struct., 322 (1994) 223.

[4] P. Carmona, M. Molina, R. Escobar, Spectrochim. Acta 49A (1993) 1.

[5] S. Hildbrand, A. Blaser, S.P. Parle, C.J. Leman, J. Am. Chem. Soc., 119 (1997) 5499.

[6] D. Gandolfo, J. Zarembowitch, Spectrochim. Acta 33A (1977) 615.

[7] T.K.K. Srinivasan, J. Mol. Liquids, 26 (1983) 177.
[8] O.P. Lamba, J.S. Parihar, H.D. Bist, Y.S. Jain, Indian J. Pure Appl. Phys.,21 (1983)236.
[9] Reena Rastogi, Ph.D. Thesis (Botony), C.C.S. Univ., Meerut (2003).
[10] R.K. Sharma, Good Manufacturing practices for ISM, Pharmaceuticals, science technology, entrepreneur, 10(18): 6(1990).
[11] NIOSH and International agency for research on cancer. IARC monographs on the evolutions of carcinogenic risks to Humans, Printing processes and Printing inks, carbon black and some Nitro compounds, Vol. 65, Lyon, Francel ARC (1996).
[12] The International pharmacopeias, Vol. 5, tests, methods and general requirements, W.H.O. Genevapub. Division (2004).
[13] Basic tests for drugs, W.H.O. Geneva- Pub. Division (2004).
[14] Official methods of analysis of the AOAC chemists, edited by K. Helrich, AOA Arlington (U.S.A.)-(2003).
[15] Official methods of microbiological analysis AOAC group, Vol. 1-3, AOAD, Arlington (U.S.A.)-(2003).
[16] The Compendium of analytical methods, Vol. 1-4, evaluation division, bureau of microbiological hazards, food directorate, Health product and food branch, Health Dept., Canada (2003).
[17] Official methods of microbiological analysis food, Vol. I, evaluation division, Health Dept., Canada (2003).
[18] Alper, Stanley, manual for therapeutics, J.W. Pub., N. York (1998).
[19] P. Pulay, G. Fogarasi, G. Pongor, J.E. Boggs, A. Vargha, J. Am. Chem. Soc. 105 (1983) 7037.
[20] M.J. Frisch, G.W. Trucks, H.B. Schlegal, GAUSSIAN 09, Revision A.02, Gaussian, Inc., Wallingford, CT, 2009.
[21] T. Sundius, J. Mol. Struct., 218 (1990) 321.
[22] T. Sundius, Vib. Spectrosc., 29 (2002) 89.
[23] MOLVIB (V.7.0): Calculation of Harmonic Force Fields and Vibrational Modes of Molecules, QCPE Program No. 807 (2002).
[24] G. Fogarasi, X. Zhou, P.W. Taylor, P. Pulay, J. Am. Chem. Soc., 114 (1992) 8191.
[25] K. Sambathkumar, Density Functional Theory Studies of Vibrational Spectra, Homo-Lumo, Nbo and Nlo Analysis of Some Cyclic and Heterocyclic Compounds (Ph.D. thesis), Bharathidasan University, Tiruchirappalli, August 2014.
[26] K.Sambathkumar,S.Jeyavijayan,M.Arivazhagan Spectrochim. Acta A147(2015)51-66.
[27] Kuppusamy Sambathkumar Spectrochim. Acta A 147 (2015) 51-66.
[28] R.G. Parr, L.V. Szentpaly, S.J. Liu, Am. Chem. Soc., 121 (1999) 1922.
[29] P.K. Chattraj, B. Maiti, U.J. Sarkar, J. Phys. Chem. A, 107 (2003) 4973.
[30] R.G. Parr, R.A. Donnelly, M. Levy, W.E. Palke, J. Am. Chem. Soc., 68 (1978) 3807.
[31] R.G. Parr, R.G. Pearson, J. Am. Chem. Soc., 105 (1983) 7512.
[32] *D.Cecily Mary Glory*, R.Madivanane and K.Sambath kumar *Elixir Comp. Chem. 89 (2015) 36730-36741*.
[33] Inger Nahringbauer, Ake Kvick, Acta Cryst., B33 (1977) 2902.
[34] http://riodbol.base.aist.go.jp/sdbs/(National Institute of Advanced Industrial Science).